Solid state synthesis of RuNiO₃ perovskite nanomaterial as an electro-catalyst for direct alcohol (ethanol, methanol and ethylene glycol) fuel cell application

Aksha Gilbert Prince[1], Lignesh Durai[1], and Sushmee Badhulika[1*]

[1]Department of Electrical Engineering, Indian Institute of Technology, Hyderabad, 502285, India.
[*]Corresponding author: E-mail: sbadh@iith.ac.in; Telephone: +040-23018443

Supplementary Information
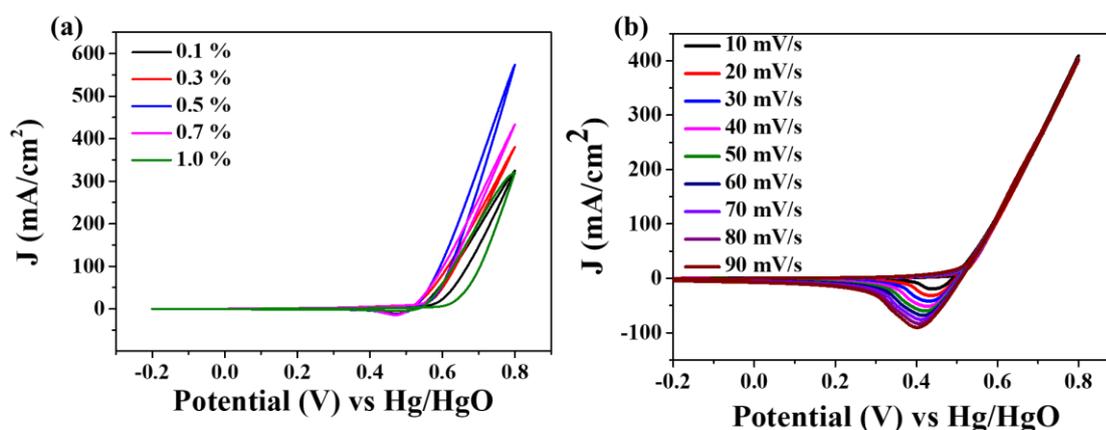
Figure. S1 (a) weight percentage optimization CV curve for 0.1 M ethanol fuel cell in alkaline medium. (b) Scan rate optimization CV for 0.1 M ethanol fuel cell in alkaline medium.

Electrochemical active surface area measurement

The ECSA measurements were carried out to understand the exact electrochemically active area of the electrode and the material. The electrochemical properties of the optimized RNO/NF electrode were analysed via a three-electrode system in the presence of 1 M KOH as a supporting electrolytic solution. Initially, the effective electrochemical active surface area of the material was examined using CV plots. Fig. S2 (a) shows the typical CV curve of NF and RNO modified NF. Here the CV curve of RNO/NF was observed with a large oxidation and reduction peak current (I_p), compared to a bare NF. The peaks identified on the CV curves can

be ascribed to the redox reaction of Ni in RNO, in line with the oxy functional groups on the surface of the material. The effective electrochemical active surface area (ECSA) was estimated via standard Randle–Sevcik equation, shown as Eqn. E1

$$\mathbf{I_{pa}\ or\ I_{pc} = 2.69\ x\ 10^5\ x\ A_e\ x\ D^{1/2}\ x\ n^{3/2}\ x\ v^{1/2}\ x\ c} \qquad \text{-------(E1)}$$

where c is the concentration of the electrolytic probe, D is the diffusion constant (7.6×10^{-6} cm^2 S^{-1}), A_e is the effective surface area, v is the scan rate of the CV curve, and n is the number of electrons involved in the redox reaction. The ECSA of RNO/NF was calculated as 0.25 cm^2 which was ~175% higher than bare NF. This enhancement in the ECSA of RNO/NF can be attributed to the lattice structuring of RNO with highly active Ni metal sites and the other oxy-functional groups adsorbed to the catalyst via Ru atoms in the lattice.

Fig. S2(b) shows the CV profiles of the optimized RNO/NF at different scan rates from 10 to 150 mV/s. The linear shifts observed in the redox potential of RNO/NF with respect to the increase in scan rate (i.e., shift toward the higher potential for oxidation peak and lower potential for reduction peak) indicates the polarization of the electrode. Fig. S2(c) displays the linear calibration curve between the log of scan rate and corresponding I_p of RNO/NF. The linear regression equations of i_{pa} and i_{pc} (inset of Fig S2(c)) with regression coefficients (R^2) of 0.980 and 0.980 show the positive correlation of the system. The slopes of i_{pa} and i_{pc} were estimated as 2.65 and 1.72 which are greater than 0.5, indicating the existence of diffusion-controlled process at the electrode surface of RNO/NF.

The chronocoulometric analysis was performed to obtain the active surface coverage of reactant ions from electrolytes onto the catalyst electrode. Fig. S2 (d) depicts the chronocoulometric analysis of bare NF and RNO/NF. The active surface coverage area was estimated using the Eqn. E2.

$$\mathbf{Q = nFA\Gamma} \qquad \text{------- (E2)}$$

where Q is the difference between reverse and forward intercepts, n is the number of transferred electrons, A is the active electrode area (1 cm^2), Γ is the active surface coverage area, and F is the Faraday constant. The Γ estimated for RNO/NF was 7.25 % higher than bare NF. This excellent augmentation in the surface coverage area of RNO/NF can be assigned to the lattice structure of RNO and the oxygen functional groups on the surface of the modified electrode
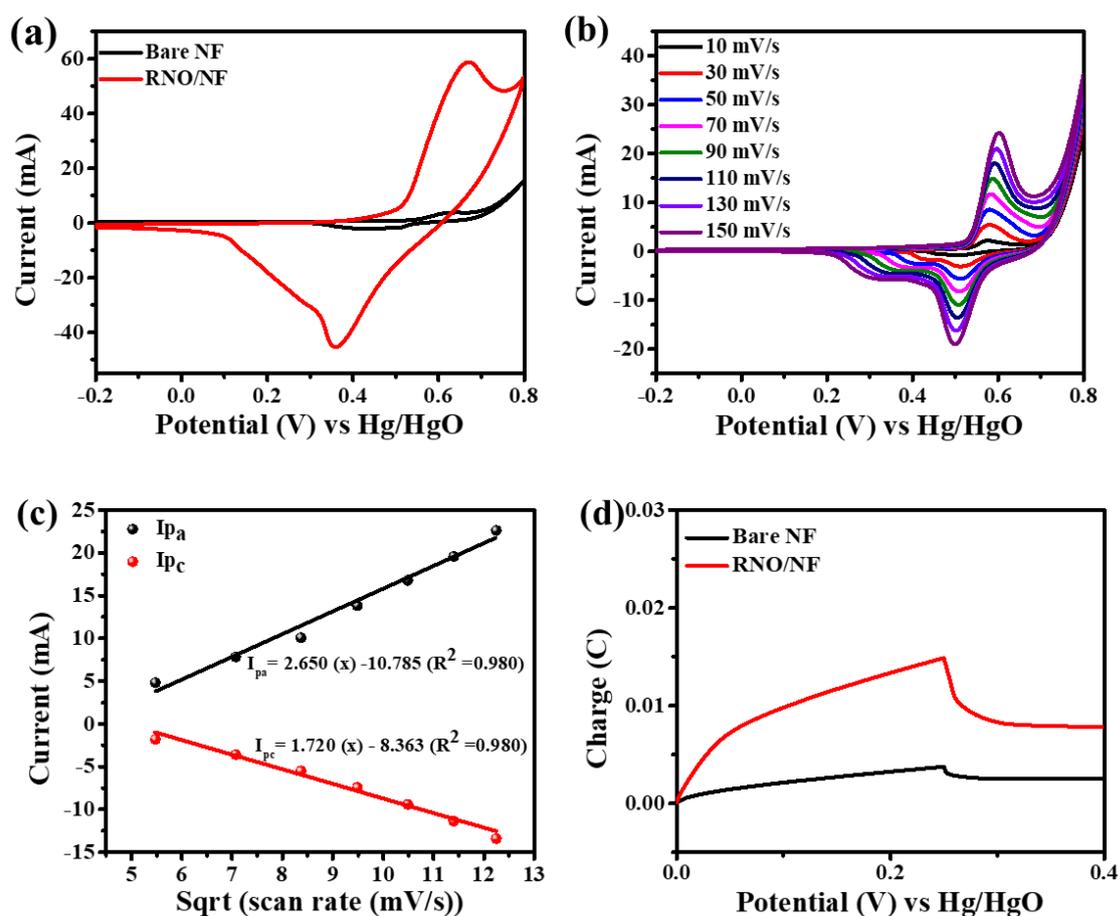
Figure S2. Electrochemical analysis in 1 M KOH electrolyte (a) CV comparison of bare NF and RNO/NF. (b) CV of RNO/NF at different scan rates ranging from 10 mV/s to 150 mV/s. (c) corresponding calibration curve (anodic and cathodic peak current vs square root of scan rate) (d) Chronocoulometric curves of bare NF and RNO/NF.

(a) Y = 777.18 (x) + 414.19 ; (R^2 = 0.9936)

(b) Y = 433.33 (x) + 344.31 ; (R^2 = 0.999)

(c) Y = 244.87 (x) + 28; (R^2 = 0.997)
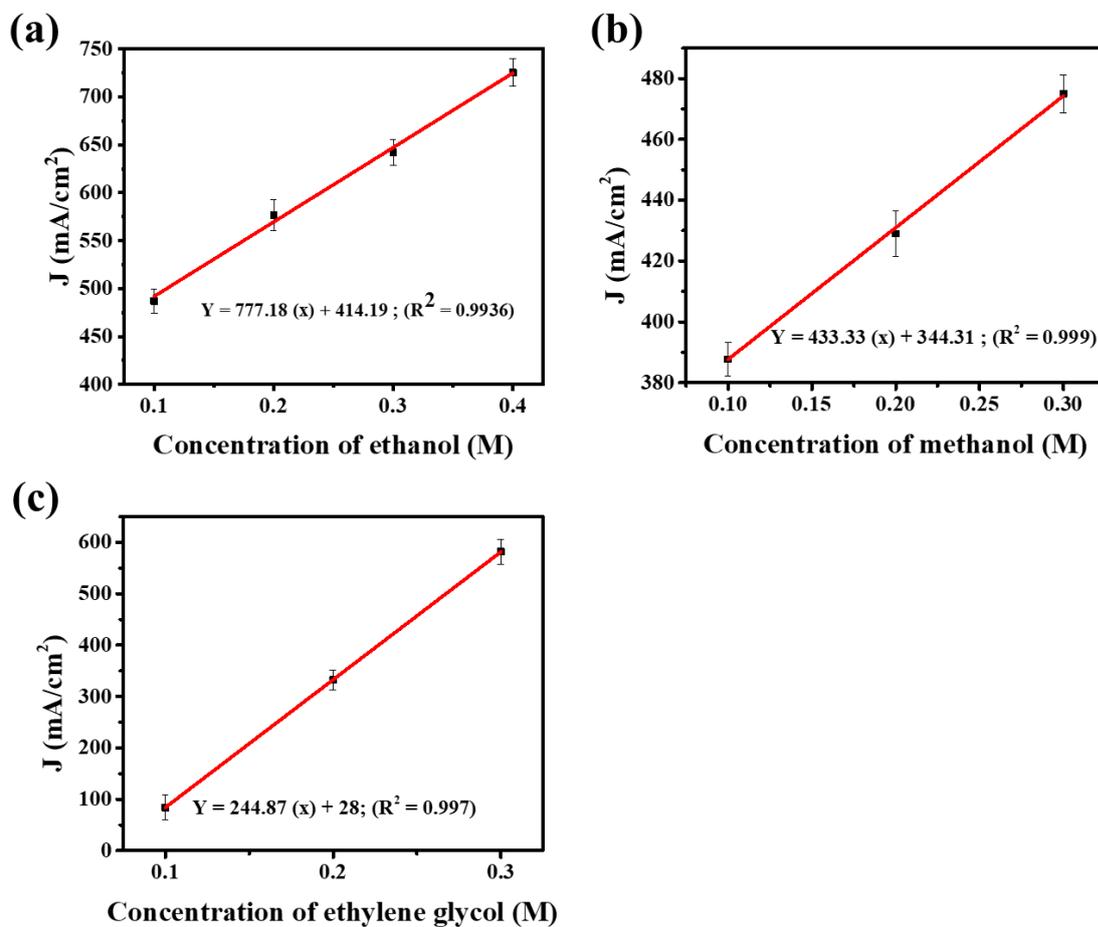
Figure. S3 Linear calibration plot for response of RNO/NF catalyst electrode to varying (a) ethanol (b) methanol and (c) ethylene glycol concentrations (for N=4 devices).

EIS Measurements:
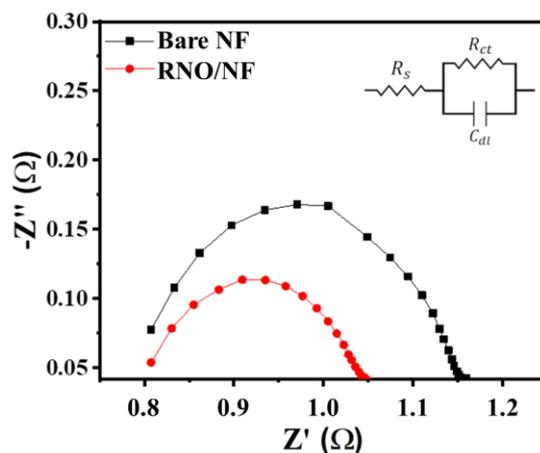
Figure. S4. Impedence spectroscopic data for bare NF and RNO coated NF in alkaline KOH solution

The measurement was carried in 1M alkaline KOH medium using bare NF and RNO coated NF as the working electrodes with Hg|HgO as the reference electrode and platinum wire as the counter electrode. From the graph, it can be concluded that the RNO electrocatalyst coated nickel foam electrode shows much higher electrocatalytic performance than bare NF.

The charge transfer resistance of the material R_{ct} is denoted by the radius of the semicircle and the R_s value denotes the electrolyte resistance. It could be analyzed that both the materials exhibited very low R_{ct} values indicating very low material resistances. Moreover, the electrolyte resistance R_s was calculated to be 0.8 Ω and the RNO catalyst resistance was calculated to be 0.236 Ω. The smaller the R_{ct} values means high electrocatalytic performance. Therefore, RNO exhibited a very low charge transfer resistance proving its ability to be considered as a potential catalyst for alcohol oxidation fuel cells.